scientific reports

Check for updates

OPEN

Effect of steel slag as fine aggregate on the mechanical and durability performance of concrete under acid exposure

Adnan Khan[1], Muhammad Luqman[1], Xu Jun[2], Muhammad Fahad Ullah[3], Abdullah Alzlfawi[4], Mahmood Ahmad[5,6] & Zsolt Toth[7]✉

The increasing demand for sustainable construction materials has driven research into alternative aggregates to reduce reliance on natural resources. This study comprehensively evaluates the mechanical and durability properties of concrete incorporating steel slag as a partial replacement for fine aggregates at replacement levels of 0%, 25%, 50%, 75%, and 100%. An extensive experimental program was conducted to evaluate compressive, tensile, flexural, and shear strengths, as well as acid resistance and microstructural stability using XRD. The results show that a 50% slag replacement achieved optimal mechanical performance, with the highest compressive and flexural strengths, improved tensile capacity, and superior shear resistance. Specifically, the 50% slag mix demonstrated a 7.9% increase in flexural strength (from 1090.7 psi to 1164.3 psi), maintaining over 82% of the compressive strength of the control at 28 days. The 25% and 75% mixes also demonstrated balanced strength and ductility characteristics. XRD analysis showed that slag-blended concretes retained key hydration products such as Calcium silicate hydrate (C-S-H) and Quartz after exposure to sulfuric acid, indicating improved chemical resistance. A newly proposed durability index, integrating both mass loss and strength retention, was used to quantify durability performance, with the 50% mix exhibiting a durability index DI_{2p} of 84.3%, significantly higher than the control's 73.8%, confirming that slag incorporation improves both mechanical and chemical resilience. These findings underscore the potential of steel slag, particularly at 25–50% replacement levels, as a sustainable and high-performance alternative to natural sand in concrete production, contributing to eco-friendly construction practices and enabling the development of more durable concrete for aggressive environments and critical infrastructure applications.

Keywords Steel slag, Compressive strength, Flexural strength, Shear strength, X-ray diffraction (XRD), Concrete durability, Sustainable construction

Concrete, as the most widely used composite building material, is composed of cement, water, and fine and coarse aggregates. Aggregates contribute to 60–75% of the total volume of concrete, with fine aggregates forming roughly 35%. These fine aggregates are critical in achieving a dense packing of the aggregate mix, which minimizes voids and reduces cement paste requirements, leading to improved stability and reduced production costs[1,2]. However, the reliance on natural aggregates, especially sand, has led to significant environmental challenges, including the depletion of natural resources and increased ecological degradation[3].

Previous research has demonstrated the feasibility of incorporating industrial by-products into concrete mixtures. For instance, studies on copper slag and blast furnace slag showed improvements in compressive strength at moderate replacement levels, with diminishing returns or reduced performance at higher percentages[4–6]. Similarly, fly ash has been used successfully as a partial replacement for both cement and

[1]Department of Civil Engineering, Tongji University, Shanghai 200092, China. [2]Department of Bridge Engineering, Tongji University, Shanghai 200092, China. [3]Department of Disaster Mitigation for Structures, Tongji University, Shanghai 200092, China. [4]Department of Civil and Environmental Engineering, Majmaah University, Al Majmaah 11952, Saudi Arabia. [5]Department of Civil Engineering, University of Engineering and Technology (Bannu Campus), Bannu 28100, Pakistan. [6]Institute of Energy Infrastructure, Universiti Tenaga Nasional, Kajang 43000, Malaysia. [7]Faculty of Wood Engineering and Creative Industries, University of Sopron, Sopron 9400, Hungary. ✉email: toth.zsolt@uni-sopron.hu

fine aggregates, improving strength and durability properties at optimal replacement levels[7]. In recent years, supplementary cementitious materials (SCMs) derived from industrial byproducts have gained widespread use as partial replacements for Ordinary Portland Cement (OPC). Among the most extensively studied SCMs are granulated blast furnace slag[8], rice husk ash[9], sugarcane bagasse ash[10], and silica fume[11], all of which exhibit pozzolanic properties. Research has demonstrated that incorporating these materials into concrete mixtures can lead to notable enhancements in mechanical performance. Recent advances in sustainable civil engineering include enhanced methods for evaluating material adhesion, seismic strengthening of existing infrastructure, and eco-composites for marine construction[12–14].

Recent studies underscore the efficacy of supplementary cementitious materials (SCMs) and fibers in enhancing alkali-activated concrete (AAC). Maganti et al. (2025)[15] demonstrated that silica fume and hybrid fibers (polypropylene/steel) significantly improve compressive strength, crack resistance, and energy absorption in alkali-activated hybrid fiber-reinforced systems. These findings align with the objectives of our research, which explores the use of steel slag, a by-product of the steel industry, as a sustainable replacement for fine aggregates[16,17]. While prior work has emphasized conventional SCMs and fibers, this study extends this paradigm by utilizing steel slag to simultaneously enhance mechanical properties, durability, and sustainability, thereby contributing to the valorization of waste materials in high-performance AAC applications.

To mitigate these challenges, researchers have investigated various waste materials and industrial by-products as potential substitutes for natural aggregates. By-products from the mining, metal, and mineral industries, such as slag and fly ash, have been widely studied for their potential to enhance concrete properties while promoting sustainability[3,18–27]. Recent research advances in sustainable construction materials include the rheological optimization of 3D printable concrete to reduce waste[28], the utilization of calcareous sand for durable marine geotechnical applications[29], and the development of energy-efficient cement composites with enhanced thermal performance and frost resistance[30]. A sustainable approach in modern construction is demonstrated through the development of high-strength concrete composite utilizing agro and industrial wastes[31–34]. Among these materials, steel slag, a by-product of steel manufacturing, has gained attention due to its favorable properties and abundance.

Steel slag, produced at a rate of 12–20% of crude steel output[35], represents a significant opportunity for recycling in construction. The World Steel Association reported a global crude steel production of 1878.5 million tons in 2022[36], producing an estimated 225 million tons of steel slag annually. For instance, China's steel slag inventory surpassed 1468 million tons in 2020 and continues to grow at over 100 million tons annually[37–39]. Without effective recycling strategies, this waste is typically landfilled or stockpiled, consuming valuable land resources and posing serious environmental risks[40]. Figure 1 illustrates the environmental threat posed by unutilized steel slag, emphasizing the urgent need for its repurposing.

Efforts to recycle steel slag in construction materials, particularly concrete, align with global sustainability goals by reducing landfill waste and lowering the carbon footprint of aggregate sourcing. Steel slag's chemical composition, primarily silicon dioxide (SiO_2) and iron oxide (Fe_2O_3), contributes positively to the hydration process, potentially improving mechanical properties such as compressive, tensile, and flexural strength[41].

Beyond mechanical performance, the durability of concrete in aggressive environments is paramount for the longevity of infrastructure. Concrete structures are frequently exposed to various forms of chemical attack, with acid exposure being a significant degradation mechanism in numerous real-world scenarios. These include industrial facilities such as chemical processing plants and wastewater treatment systems, agricultural settings (e.g., silage pits), and urban environments affected by acid rain or chemical spills. Acid attack leads to the

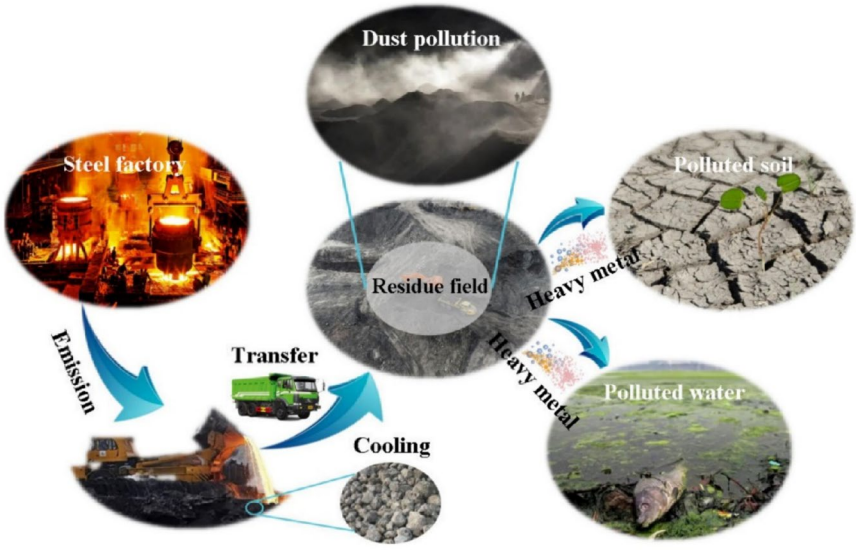

Fig. 1. Environmental threat of unutilized steel slag[38].

dissolution of calcium-bearing phases in the cement paste, increased porosity, and ultimately, loss of strength and structural integrity[42–45]. Therefore, assessing the resistance of steel slag concrete to acid exposure is crucial for its confident application in demanding service conditions and ensuring long-term performance.

Current research highlights that incorporating steel slag as a partial replacement for fine aggregates can significantly enhance concrete performance. Optimal replacement levels, typically ranging from 30% to 45%, have been shown to improve compressive strength across various curing periods. The chemical composition of steel slag, which includes compounds such as silicon dioxide (SiO_2) and iron oxide (Fe_2O_3), plays a crucial role in this enhancement by contributing positively to the hydration process. This, in turn, improves the overall strength and durability of concrete structures[46].

Although numerous studies have investigated the use of steel slag as a replacement for natural aggregates in concrete, most have focused on partial substitution levels (typically 30–45%) and primarily evaluated compressive strength and chloride permeability[47]. Few have examined the full spectrum of mechanical and durability responses across a broader replacement range. Furthermore, prior research often omits tensile, shear, and post-peak flexural behaviours or provides limited discussion of acid resistance mechanisms.

Despite the growing interest in incorporating industrial byproducts, such as steel slag, into concrete formulations, substantial gaps persist in understanding the full range of their impacts on the mechanical and durability characteristics of concrete. Existing research has predominantly concentrated on parameters such as compressive strength and chloride resistance, while the investigation of additional properties, including tensile, flexural, and shear strength, remains comparatively limited. Moreover, most studies have employed moderate levels of slag replacement (30–60%), leaving the implications of elevated replacement levels (≥ 75%) significantly under-researched. Furthermore, there is a notable deficiency in thorough durability assessments, particularly concerning chemical exposures such as sulfuric acid. This study aims to fill these voids by evaluating a wider range of slag replacement levels (0-100%) and proposing an innovative composite durability index that integrates both mass loss and strength retention upon exposure to acid.

Research objectives

The current study aims to critically assess the potential of utilizing steel slag as a sustainable partial substitute for fine aggregates in the production of sustainable concretes, with a special focus on their strength properties and durability parameters. In particular, its precise objectives were to:

- Investigate the impact of various percentages of replacement of steel slag (0%, 25%, 50%, 75%, 100%) upon compressive strength, splitting tensile strength, flexural strength, and shear strength of the concrete.
- Evaluating the durability performance after being exposed to sulfuric acid and devising a novel composite durability index (DI_{2p}) with both mass loss retention and strength retention.
- Characterize the microstructural constitution and phase stability using X-Ray Diffraction (XRD) analysis to understand the relationship between microstructural changes and macro-scale function.

Novelty and contribution

This research study presents a comprehensive evaluation of steel slag as a sustainable alternative to fine aggregate in concrete, exploring an extensive, yet underexplored, spectrum of replacement levels ranging from 0% to 100%. This work provides novel mechanical and durability performance data for high-volume slag replacements (75% and 100%), addressing a significant gap in existing literature. A key innovation is the development of a composite durability index (DI_{2p}) that integrates mass loss and strength retention metrics, offering a more comprehensive assessment of concrete performance under sulfuric acid attack. Furthermore, XRD microstructural analysis reveals the phase stability mechanisms underlying the observed macro-scale performance in aggressive environments. Together, these contributions advance the understanding of steel slag as a sustainable, high-performance alternative to natural sand, demonstrating its potential to enhance both the durability and environmental profile of concrete production.

Methods and materials

This section outlines the materials, mix design, specimen preparation, and testing procedures employed to evaluate the effectiveness of steel slag as a fine aggregate substitute in concrete. The research focuses on examining the mechanical properties of concrete, including compressive, tensile, flexural, and shear strength, by replacing fine aggregates with steel slag in varying proportions. The experimental program was designed to systematically capture the behavioral response of concrete across a wide spectrum of steel slag replacement ratios. Four substitution levels were selected (25%, 50%, 75%, and 100%) based on the weight of fine aggregate. This approach addresses the critical range of 30–60% identified in prior research[47], while also exploring under-studied configurations at 25% and 75%, which may exhibit nonlinear mechanical or durability trends. Unlike earlier works that predominantly assessed 30–45% replacement, this extended matrix enables a more comprehensive understanding of the threshold effects, strength plateauing, or sudden deterioration observed particularly at high slag dosages[46]. The inclusion of the 100% mix further investigates the upper limit of substitution feasibility, crucial for sustainable waste valorization in high-volume applications.

The methodology begins with a comprehensive characterization of the materials, including Portland cement, water, coarse and fine aggregates, and steel slag, to establish their suitability for concrete production. A mixed-design was developed in Fig. 2 following ACI-211, ASTM C192/C192M-23 guidelines to achieve a target compressive strength of 3000 psi. The experimental program involved casting in Table 1. Immediately after casting, specimens were covered with plastic sheets to prevent moisture loss and demolded after 24 h. Subsequently, all specimens were cured by immersion in a water tank maintained at a temperature of 23 ± 2 °C until the designated testing ages (3, 7, and 28 days), and a total of 60 specimens (30 cylinders and 30 beams) were

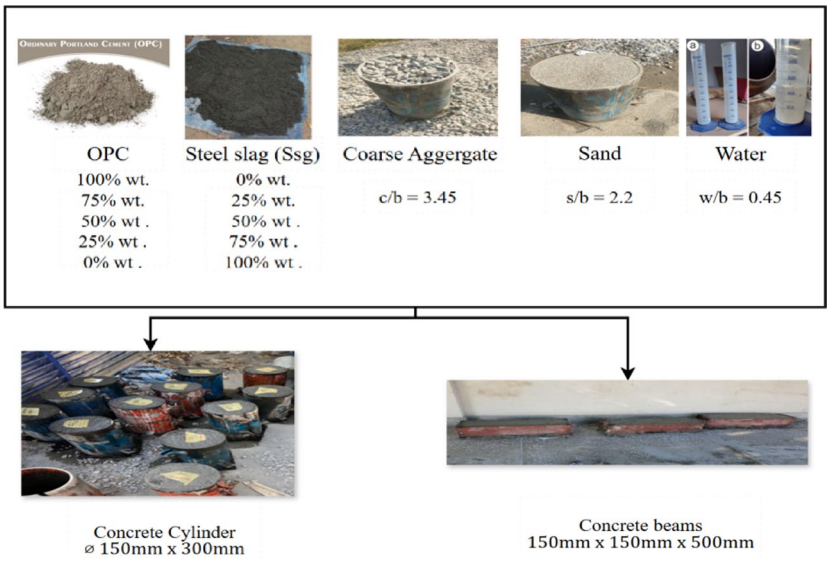

Fig. 2. Design of concrete containing steel slag.

Specimen	Test type	Age of testing (days)	Control (0%)	25%	50%	75%	100%	Total
Cylinder	Compression	28	3	3	3	3	3	15
Cylinder	Splitting Tensile	28	3	3	3	3	3	15
RC Beam	Compression	28	3	3	3	3	3	15
RC Beam	Splitting Tensile	28	3	3	3	3	3	15

Table 1. Casting plan for cylinders and beams.

tested under various loading conditions. Both destructive and non-destructive tests were performed to evaluate the performance of the concrete specimens, with particular emphasis on understanding the influence of steel slag replacement on the mechanical properties and overall quality of the concrete.

Cement

Ordinary Portland Cement of grade 43, which complies with ASTM C150[48] Type I criteria were utilized in this investigation. To preserve freshness and avoid moisture contamination, the locally obtained cement was kept in regulated storage, guaranteeing reliable performance. Approximately 20% of the volume of concrete is made up of cement, which acts as the main binding agent by filling in gaps and joining aggregates to create a strong matrix. The ideal cement content is essential, too much cement might result in shrinkage and lower quality, while too little cement produces weak concrete with more voids.

Coarse aggregate

The selection of locally sourced coarse aggregates was based on their quality and durability; they were subjected to rigorous screening and washing to remove impurities, which ensured consistency in physical properties, the gradation followed industry standards, optimizing packing density and interlocking within the concrete matrix; their excellent angularity and particle shape facilitated robust inter particle bonding, enhancing mechanical properties like compressive and flexural strength; control tests, which are detailed in, further emphasize the coarse aggregate's suitability for use in concrete formulations.

Table 2, confirmed how well the concrete mixtures worked. These tests were carried out in compliance with pertinent ASTM guidelines[49], guaranteeing precision and dependability. The well-graded quality of the coarse aggregate is further highlighted in Fig. 3, which highlights its appropriateness for use in concrete formulations. These aggregates were chosen to demonstrate a dedication to performance, quality, and longevity in concrete formulations.

Fine aggregate

To achieve optimal workability and cohesiveness in our concrete mixtures, the careful selection of fine aggregates was essential. These aggregates, which were sourced locally, were thoroughly screened and cleaned to eliminate impurities and guarantee uniformity in their physical characteristics. Optimal particle packing within the concrete matrix was promoted by grading that complied with industry standards[50]. As shown in Table 3, control tests were carried out to confirm the concrete formulations. To ensure accuracy and dependability in evaluating the fine aggregates quality, the tests were conducted in compliance with pertinent industry standards. The fine

S.NO	Characteristic	Value
1	Type	Crushed 1 inch
2	Specific Gravity	2.67
3	Average rodded density	1876.39 kg/m^3
4	Total Water Absorption	1.41%
5	Moisture Content	0.89%
6	Fineness modulus	6.75

Table 2. Physical properties of coarse aggregates.

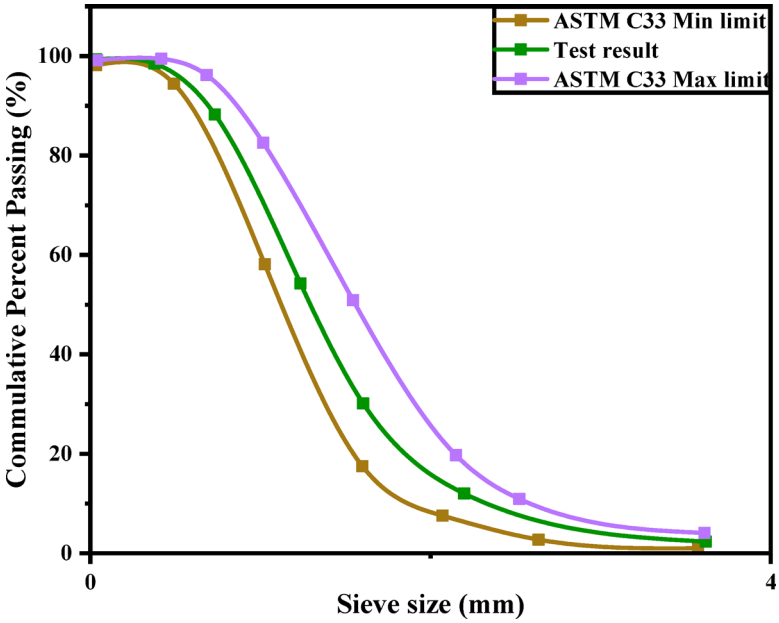

Fig. 3. Gradation of coarse aggregates.

S.NO	Characteristics	Value
1	Type	Uncrushed (natural)
2	Specific gravity	2.65
3	Average rodded density	1753.43 kg/m3
4	Total Water Absorption	1.08%
5	Moisture Content	0.18%
6	Fineness Modulus	2.72

Table 3. Physical properties of fine aggregate.

aggregates' well-graded nature is further demonstrated in Fig. 4, which highlights their appropriateness for use in our concrete mixtures.

Steel slag

Steel slag has a wide spectrum of industrial applications, especially in construction, cement manufacturing, and environmental management, contributing significantly to circular economy principles by valorising an industrial by-product[51]. Its high density, angular shape, excellent abrasion resistance, and mechanical stability make it a valuable aggregate substitute in road construction, asphalt mixtures, and concrete[52]. Tables 4 and 5 provide an overview of the physical and chemical properties of the steel slag utilized in our study. These properties were essential in evaluating the impact of steel slag on the performance and characteristics of the concrete mixtures. Figure 5 further illustrates the results of comparing various aggregates of a well-graded nature, highlighting their suitability for use in our concrete composition.

Before its use in concrete, the steel slag underwent a crucial pre-treatment process involving natural weathering and aging for a minimum of six months. This common practice for steel slag helps to mitigate

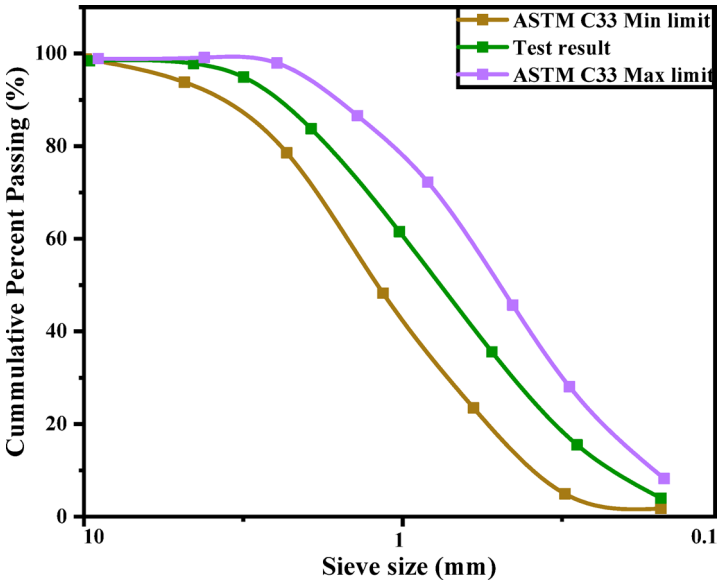

Fig. 4. Gradation of fine aggregates.

S. no	Characteristics	Value
1	Specific gravity	3.23
2	Average rodded density	1796.38
3	Total Water Absorption	1.43
4	Fineness Modulus	2.42

Table 4. Physical properties of steel slag.

S. no	Element	Results in percentage %
1	Silica as SiO_2	42.05
2	Iron as Fe_2O_3	28.73
3	Manganese as MnO	10.26
4	Calcium as CaO	5.10

Table 5. Chemical composition of steel slag.

potential volume instability caused by the hydration and carbonation of expansive compounds such as free lime (f-CaO) and magnesium oxide (MgO), which are typically present in fresh slag[51]. This aging process ensures the long-term dimensional stability and durability of the concrete by allowing these reactive compounds to hydrate or carbonate before being incorporated into the mix.

Table 5 presents the detailed chemical composition of the steel slag utilized in this study, determined through X-ray fluorescence (XRF) analysis. The primary constituents include silica (SiO_2: 42.05%), iron oxide (Fe_2O_3: 28.73%), manganese oxide (MnO_2: 10.26%), and calcium (CaO: 5.10%). The significant presence of silica and calcium oxides suggests latent hydraulic properties, contributing to the formation of additional calcium silicate hydrate (C-S-H) gel over time, which enhances the concrete's mechanical properties and microstructure[49]. Understanding this chemical profile is fundamental for confidently assessing steel slag's reactivity and its long-term performance in concrete applications.

As detailed in Tables 3 and 4, the steel slag fine aggregate exhibited a higher specific gravity (3.23) and a slightly lower fineness modulus (2.42) compared to the natural fine aggregate (2.65 and 2.72, respectively). Furthermore, the steel slag particles are inherently more angular and possess a rougher surface texture compared to the typically rounded natural sand particles (as visually implied by Fig. 5, which compares sieve analyses). This distinct morphology significantly influences the concrete's properties. The angularity of steel slag promotes enhanced mechanical interlock between aggregate particles within the concrete matrix, which can contribute to improved packing density and reduce void content. Moreover, the rough surface texture provides a larger effective surface area for adhesion, leading to a stronger and denser interfacial transition zone (ITZ) between the slag particles and the cement paste[49]. This improved ITZ, characterized by better bond and reduced porosity,

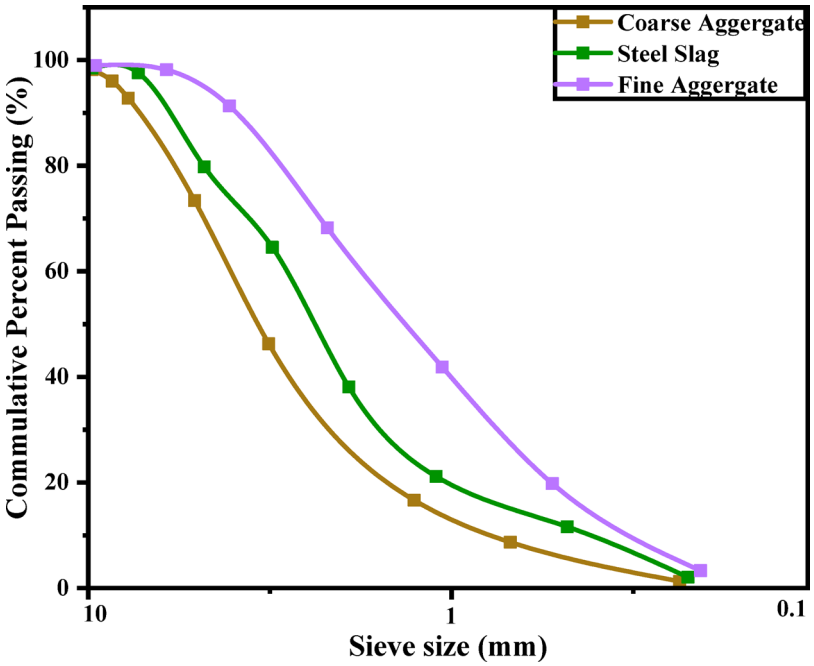

Fig. 5. Sieve analysis results comparison.

Fig. 6. Measurement of workability using the slump cone apparatus.

is a key factor contributing to the observed enhancements in mechanical properties, particularly flexural and shear strengths.

Test procedure

Workability

Workability describes the ease of mixing, transporting, moulding, and compacting concrete by measuring the internal energy needed for full compaction. The energy required to overcome friction during compression affects this characteristic. Concrete is compacted in three layers for the slump test, which is conducted using a slump cone with dimensions of 20 cm for the bottom diameter, 10 cm for the top diameter, and 30 cm for the height. A conventional tamping rod, 60 cm long and 16 mm in diameter is used to tamp each layer 25 times. The slump is the amount of concrete that sinks under gravity, expressed in millimetres. Figure 6 illustrates how to use a slump cone instrument to measure workability. All reported means are from $n = 3$ specimens; error bars show ± 1 SD unless noted.

Compressive strength (CS)

In compliance with ASTM C39/C39M[53] standard procedures, compressive strength was assessed using cylindrical specimens that were 150 mm in diameter and 300 mm in height. A total of 60 cylinders were cast for this purpose, with five categories of steel slag replacement in fine aggregates: 0% (control), 25%, 50%, 75%, and 100%. Each category consisted of 12 cylinders, including three replicates for compressive strength, three for

splitting tensile strength, and six for flexural performance, ensuring statistical reliability and repeatability of the results. Following casting, all specimens were cured in water for 28 days in a controlled laboratory setting. A Universal Testing Machine (UTM) was used to perform the compressive strength test, applying a uniaxial load continuously until failure occurred. The Universal Testing Machine (UTM) used for testing concrete cylinders to determine compressive strength is shown in Fig. 7a. The contour and 3D surface plots were generated in Excel to visually illustrate the interaction between slag replacement levels and their influence on the measured property. These plots are based solely on the experimental data points and are intended for qualitative understanding rather than predictive modelling.

Flexural strength (FC)
Flexural strength testing was carried out at 28 days to assess the bending resistance of concrete incorporating varying proportions of steel slag as a fine aggregate replacement. The procedure adhered to ASTM C293[54], which involves a centre-point loading configuration. In this method, each beam specimen was supported at two ends while a concentrated load was applied precisely at mid-span, inducing flexural stress. The loading was applied gradually until structural failure occurred, and the peak load was recorded for strength calculation. For this investigation, a total of 30 concrete beams were prepared, representing five replacement levels of fine aggregate with steel slag: 0% (control), 25%, 50%, 75%, and 100%. For each mix ratio, three beams were cast to ensure consistency and experimental reproducibility. The test setup, illustrated in Fig. 7b, utilized a Universal Testing Machine (UTM) to apply the central load and monitor the response. This configuration allowed for a reliable evaluation of the beam's capacity to resist flexural failure, offering insight into the effectiveness of steel slag as a sustainable alternative to natural sand in structural applications. The contour and 3D surface plots were generated in Excel to visually illustrate the interaction between slag replacement levels and their influence on the measured property. These plots are based solely on the experimental data points and are intended for qualitative understanding rather than predictive modelling.

Splitting tensile strength (T)
Splitting tensile strength testing was conducted at 28 days in accordance with ASTM C496 to evaluate the indirect tensile capacity of concrete incorporating different percentages of steel slag as a fine aggregate replacement. This method involves placing cylindrical specimens horizontally in a Universal Testing Machine (UTM) and applying a compressive load along the vertical diameter of the cylinder in Figure 8a, inducing tensile stresses perpendicular to the direction of loading. The applied load was steadily increased until the specimen failed by splitting along its vertical axis. Three specimens from each mix category 0%,25%,50%,75% and 100% steel slag replacement were tested to ensure consistency. The maximum load at failure was recorded and used to compute the splitting tensile strength using the standard formula prescribed in ASTM C496[55]. This test provided valuable insight into the tensile behaviour of concrete when natural sand is partially or fully substituted with steel slag.

Shear strength (Vc)
Shear strength testing was performed at 28 days to evaluate the ability of concrete beams to resist shear forces when fine aggregate was replaced with varying percentages of steel slag. The procedure followed the principles outlined in ASTM C496[55], adapted for beam specimens to simulate shear failure conditions. In this method, beams were positioned in a Universal Testing Machine (UTM) in Fig. 8b, and a concentrated load was applied near the supports to induce shear stress. The load was gradually increased until failure occurred, and the peak load was recorded. Three specimens from each replacement level, 0%,25%,50%,75% and 100% steel slag, were tested to ensure consistency. The maximum load at failure was used to calculate the shear strength based on the beam's cross-sectional area. This test enabled an effective comparison of shear performance across different

Fig. 7. (**a**) Compressive strength test (**b**) Flexural strength test.

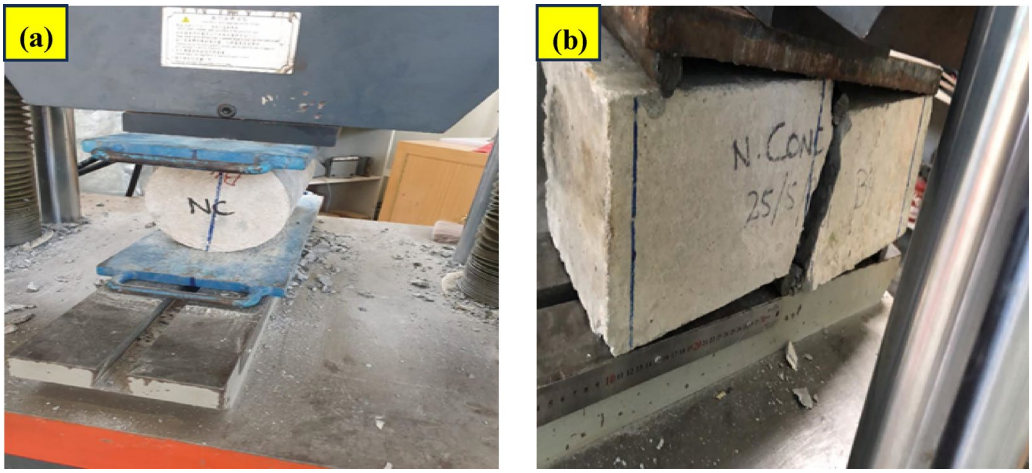

Fig. 8. (**a**) Splitting tensile test (**b**) Shear strength test.

slag replacement levels, offering insights into the structural viability of steel slag as a fine aggregate substitute. The contour and 3D surface plots were generated in Excel to visually illustrate the interaction between slag replacement levels and their influence on the measured property. These plots are based solely on the experimental data points and are intended for qualitative understanding rather than predictive modelling.

X-ray diffraction (XRD)

Concrete's strength depends on the formation of a microstructure that connects all its particles. XRD is an analytical technique that determines the crystalline structure of materials by directing X-rays at the material and measuring the angles and intensities of the diffracted beams. XRD provides detailed information on the crystal structures, phases, preferred crystal orientations, and other structural characteristics like average grain size, crystallinity, strain, and crystal defects[56]. The atomic arrangement of a material can be interpreted by analysing the intensity of the peaks in the XRD pattern, which reveals the atomic distribution within the lattice structure. Cement, the reactive binder phase in concrete, hydrates to generate this microstructure[57]. A few well-established techniques compute the areas under the respective XRD curves to ascertain the degree of crystallinity in materials. These techniques presume that one component of the XRD pattern is amorphous, and the other is crystalline. In subsequent analysis, the computed areas are thus regarded as proportionate to the volumes of the corresponding phases[58,59].

Acid exposure testing

To evaluate the durability performance under aggressive chemical attack, concrete specimens were subjected to acid exposure. Acid resistance was evaluated on cylinders cast from the same batches as the mechanical tests. Beams were not immersed (reserved for flexural/shear tests). After 28 days of initial curing of the samples in water, designated cylindrical specimens were fully immersed in aqueous sulfuric acid (H_2SO_4) at 23 ± 2 °C. The solution concentration was prepared to achieve a pH of 1, consistent with an ASTM C267 type procedure. The acid solution was replaced with a fresh solution at each measurement interval (0, 28, 56, 90, and 120 days) to maintain a severe and reproducible aggressive environment. This routine solution renewal ensures constant aggressiveness throughout the exposure period, mirroring sulphuric-acid programs that use ASTM C267 indicators (mass, dimensions, strength) and routine solution renewal[43,44]. In addition to solution renewal at scheduled intervals, the acid bath pH was checked at least once daily and adjusted with fresh H_2SO_4 to hold pH (1.0). Daily control is standard in severe sulfuric acid durability programs to maintain constant aggressiveness throughout exposure. The total exposure duration for some tests extended up to 120 days, while for the durability index calculation, relevant data points were utilized within this timeframe. This rigorous approach simulates an accelerated degradation process representative of severe acidic environments encountered in industrial settings, wastewater treatment facilities, and areas prone to acid rain, allowing for a comparative assessment of the materials' long-term performance under aggressive conditions. Mass changes were monitored following ASTM C267, and compressive strength of exposed cylinders (when strength retention was required) followed EN 12390-3.

Durability index

ACI 201.2[60] states that durable concrete must maintain its form, serviceability, and quality in the environment. According to the research background, researchers have evaluated the durability of concrete in an acidic environment based on either one parameter (such as compressive strength) or, in the case of multiple parameters, their effects have not been considered simultaneously. Wang et al.[61] evaluated the durability in a sulfuric acid environment by taking into consideration the mass change parameter, while Hendi et al.[62] presented a relation to compare the durability of different mixtures in a magnesium sulphate environment by concurrently considering only three parameters (compressive strength, mass change, and volume change. In this study, a novel Durability

Index (DI) was developed to evaluate the overall performance of steel slag concrete. Under sulphuric-acid attack, concretes may lose mass (erosion) and mechanical capacity (decalcification). To avoid single-metric bias, we report a two-parameter, dimensionless durability index (DI_{2p}) combining mass loss and compressive-strength retention measured on companion cylinders. The index is used only as an internal comparator across the replacement levels.

Measurements (cylinders).

- Initial (before immersion): cylinder mass m_0 and compressive strength $f_{c,0}$ at 28 d.
- After immersion at a common exposure age t_n: cylinder mass m_n and compressive strength $f_{c,n}$.
- Keep exposure time t_n identical for all mixes.

$ML = \frac{m_0 - m_n}{m_0}$ (0≤ML≤1) (fractional mass loss).

$SR = \frac{f_{c,n}}{f_{c,0}}$ (0 ≤ SR≤1) (fractional strength retention).

Durability Index (this study).

DI_{2p} (%) = 100 SR (1 − ML).

A larger DI_{2p} indicates better overall durability within this test program. For transparency, we always report the component metrics ML and SR (mean ± SD or 95% CI) alongside DI_{2p}.

Results and discussion

This section presents the experimental results obtained from laboratory testing of concrete incorporating varying percentages of steel slag as a fine aggregate replacement. Compressive strength, splitting tensile strength, flexural strength, and shear strength were evaluated at 28 days to investigate the mechanical behaviour of each mix. The correlation between slag content and strength parameters was analyzed to assess the influence of slag on structural performance. The findings are discussed in detail in the following sections.

Workability

Workability of concrete mixes was evaluated through slump testing, and the results are shown in Fig. 9. With a constant water cement ratio of 0.45, the control mix (100% sand) exhibited the highest slump value of 59.03 mm, while mixes with 25%, 50%,75% and 100% slag replacements showed decreased slump values of 54.18 mm,56.61 mm,54.1 mm, 47.9 mm, and 41.58 mm, respectively, in Fig. 9. This reduction is primarily due to the rough and angular texture of iron slag particles, which increases internal friction and hinders flow ability[63]. Additionally, slag's higher water absorption compared to natural sand reduces the amount of free water in the mix, further lowering workability[42]. The substitution of sand with slag also alters the overall mix proportions, potentially necessitating adjustments in the water-to-cement ratio or use of admixtures to maintain suitable workability. The slump test offers a quick assessment; it is acknowledged that a more comprehensive understanding of the fresh concrete properties, including rheological parameters such as yield stress and plastic viscosity, would provide deeper insights into pumpability, segregation resistance, and overall placement characteristics. Such detailed rheological characterization is recommended for future research to fully optimize the mix design for various practical applications.

Compressive strength (CS)

The average compressive strength values for various steel slag replacement levels (0%, 25%, 50%, 75%, and 100%) at 3, 7, and 28 days are summarized in Table 6. The control mix (0% slag) exhibited the highest compressive strength of 2940.20 psi at 28 days, followed by decreasing values as the replacement level increased, as presented in Fig. 10. The 25% slag mix demonstrated only a slight reduction from the control, indicating good strength retention. The 50% and 75% slag mixes maintained moderate performance, while the 100% slag mix yielded the lowest compressive strength (2093.43 psi), consistent across all curing ages. Similar trends were observed at 3 and 7 days. The incorporation of steel slag as a partial (25%, 50%, and 75%) or full (100%) replacement of fine aggregate resulted in progressive strength reductions compared to the control mix.

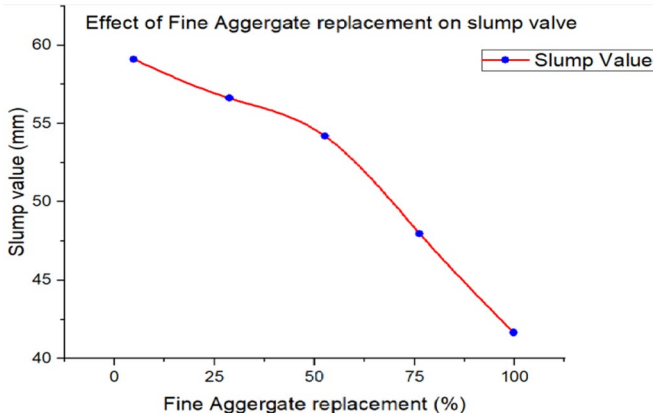

Fig. 9. Variation of slump value.

Mix	Compressive strength (psi)			Flexural Strength (psi)
	3 days	7 days	28 days	28 days
NCM (0%)	1965.45	2324.45	2940.20	1090.7
25% Slag	1815.00	2200.00	2725.00	1125.0
50% Slag	1645.52	2072.85	2410.50	1164.3
75% Slag	1600.00	1900.00	2250.00	1175.0
100% Slag	1552.63	1724.52	2093.43	1178.9

Table 6. Average compressive strength and flexural strength results.

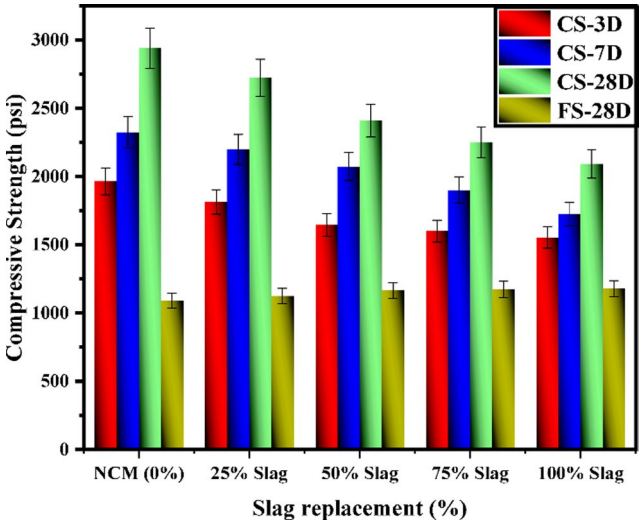

Fig. 10. Experimental results of CS and FS containing Steel slag at varying percentages.

During compressive strength testing, control specimens primarily exhibited brittle, sudden failure with prominent diagonal cracks. In contrast, concrete mixes incorporating steel slag, particularly the 50% and 75% replacement levels, showed a more ductile failure pattern, characterized by a more gradual development of microcracks and increased spalling before ultimate collapse, suggesting an enhanced ability to deform under load and better energy dissipation. This ductile behaviour is indicative of a more resilient concrete matrix due to the presence of slag.

The 25% slag mix retained approximately 93% of the compressive strength of the NCM at 28 days, indicating minimal compromise in performance. The 50% and 75% mixes retained around 82% and 76%, respectively, while the 100% slag mix maintained 71% of the control strength. These results suggest that up to 50% slag replacement is suitable for structural applications, offering a favourable balance between mechanical performance and sustainability. The reduction in strength at higher slag contents may be attributed to lower slag reactivity, increased water demand, and the rough texture of slag particles that hinder dense packing and hydration kinetics.

These results align with established research on slag-modified concrete, which suggests that optimal replacement levels typically lie below 40–60% to achieve a balance between mechanical performance and environmental benefits. Continued hydration of slag particles and the potential for pozzolanic reaction can improve strength over longer curing periods, but excessive slag may dilute cementitious content, thereby limiting strength development.

Figure 11 illustrates a contour plot showing the variation of compressive strength with slag content and curing age. The strength of concrete increases consistently with longer curing, reaching its maximum at 0% slag and 28 days (2940 psi). Partial slag replacement (25–50%) maintains competitive strength levels, particularly at 28 days, demonstrating its potential as a sustainable alternative with only moderate performance compromise. However, mixes with 75% and 100% slag show a significant reduction in strength across all curing periods. This trend supports the view that excessive slag content can dilute the cementitious matrix and slow pozzolanic reaction kinetics, resulting in poor early and late-age strength development. The data emphasize the importance of optimizing slag content below 50% to strike a balance between environmental sustainability and mechanical performance.

These findings align with previous research, which suggests that slag replacement between 35% and 60% is typically optimal in Fig. 12. The visual representation in the contour plot enhances the understanding of slag's influence over time, and the lack of strength recovery in 100% slag mixes underlines the performance limitations of full replacement strategies.

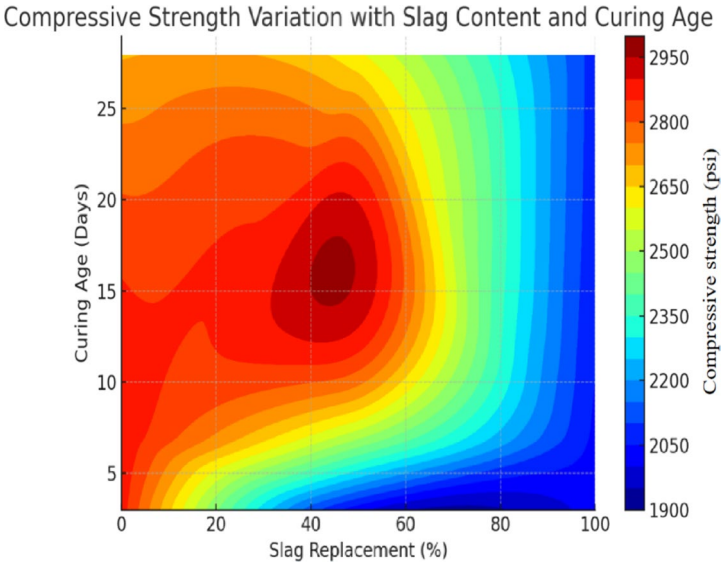

Fig. 11. Contour Plot of the CS results.

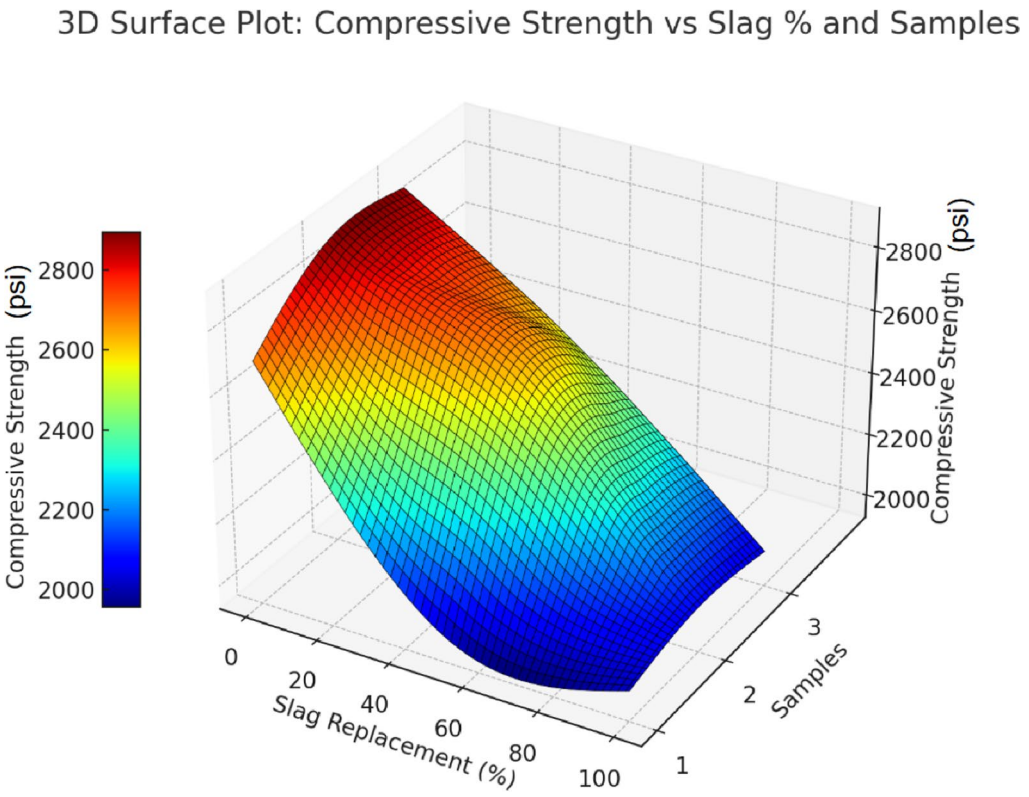

Fig. 12. 3D Surface Plot of the CS results.

Flexural strength (FS)

Flexural strength tests were conducted on concrete mixes with five different levels of steel slag replacement: 0%, 25%, 50%, 75%, and 100%, as shown in Fig. 10 and summarized in Table 6. The control mix with 0% slag (normal concrete) recorded an average flexural strength of 1090.7 psi. At 25% slag replacement, the flexural strength slightly increased to 1125.0 psi, suggesting early improvements in microstructure. With 50% slag, the strength reached 1164.3 psi, showing a clear enhancement due to better particle packing and possible pozzolanic activity. At 75% slag, the flexural strength continued to increase to 1175.0 psi, and finally, 100% slag achieved the highest value of 1178.9 psi, indicating the strongest bending resistance among all mixes. For flexural tests,

all beams exhibited typical flexural failure, initiated by tensile cracking at the bottom midspan. However, the steel slag-modified beams demonstrated a more stable crack propagation and sustained higher loads over larger deflections compared to the control. The 50% slag mix displayed significant post-peak ductility, with the ability to maintain load-carrying capacity even after initial cracking, highlighting improved toughness attributed to the enhanced aggregate-matrix bond.

These results reflect a steady upward trend in flexural strength with increasing slag content. The observed increase in flexural strength with increasing steel slag content, culminating in the highest value at 100% replacement, might appear counterintuitive given the replacement of natural aggregate. However, this phenomenon can be scientifically explained by the unique physical characteristics of steel slag. Steel slag particles possess an angular shape and a rougher surface texture compared to the smoother, more rounded natural sand (as discussed in Sect. 2.4). This morphology leads to enhanced mechanical interlocking between the slag particles and the surrounding cement paste, forming a stronger and denser interfacial transition zone (ITZ)[6]. In concrete, the ITZ is often the weakest link, and improvements in this region directly contribute to enhanced bond strength and crack resistance. Under flexural loading, the improved ITZ allows for more efficient transfer of tensile stresses, delaying crack initiation and propagation, thereby increasing the material's bending capacity. This enhanced bonding and internal friction contribute to the superior flexural performance observed even at high slag replacement levels. The continuous improvement can be attributed to enhanced interfacial bonding, secondary hydration, and dense microstructure formation. Notably, even at full replacement, slag did not hinder flexural performance but rather improved it, a critical finding for sustainability-focused construction.

However, to generalize these outcomes, further testing under varied curing times, cyclic loading, and environmental conditions is recommended. Nonetheless, this study confirms that steel slag, even at 100% replacement, can be a reliable Supplementary Cementitious Material (SCM) for applications where flexural performance is critical, as shown in Fig. 13.

Load–displacement curves

The flexural performance of the simply supported reinforced concrete beams was evaluated through mid-span load deflection responses under centre-point loading, as illustrated in Fig. 14. Each curve represents a distinct level of fine aggregate replacement using steel slag: 0%, 25%, 50%, 75%, and 100%. All specimens exhibited a typical three-stage flexural response: (i) an initial linear elastic phase governed by uncracked concrete behaviour; (ii) a nonlinear phase marked by matrix cracking, reinforcement yielding, and interfacial slip; and (iii) a post-peak softening phase indicating progressive damage and loss of load carrying capacity. Among the tested specimens, the beam incorporating 50% steel slag demonstrated the highest peak load capacity (67.4 KN) with a corresponding deflection of approximately 7.9 mm, reflecting an optimal balance between strength and ductility. The 25% and 75% replacement levels also showed enhanced ductility and adequate strength, indicating improved energy dissipation characteristics relative to the control. Conversely, the control beam (0% replacement), although reaching a peak load of 60.2 KN, exhibited a sudden load drop after cracking (7.2 mm deflection), indicating brittle failure behaviour. The 100% replacement beam attained a peak of 58.7 KN but

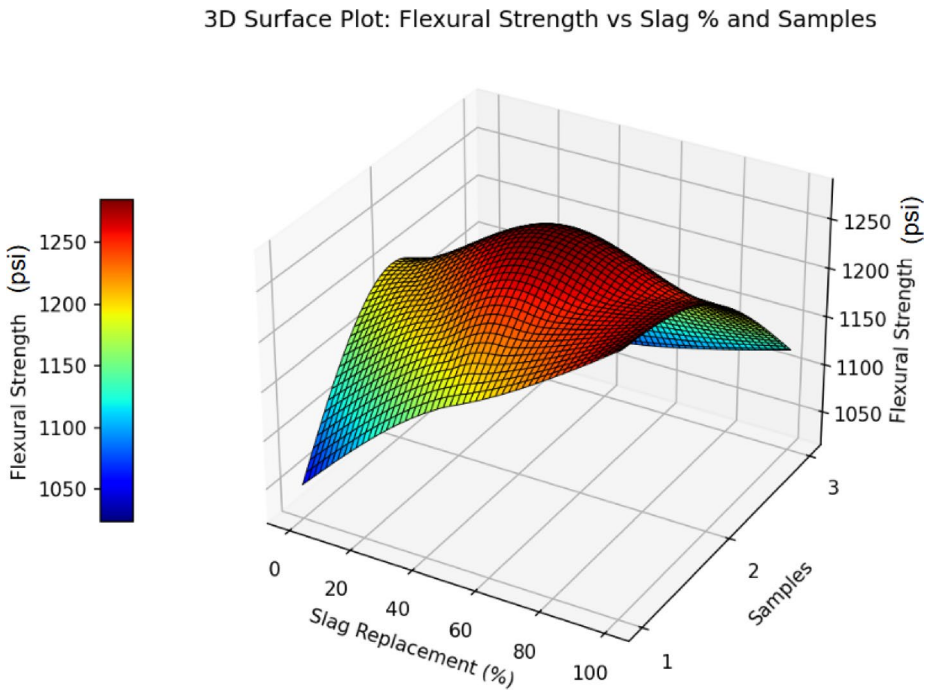

Fig. 13. The 3D surface plot of FS results.

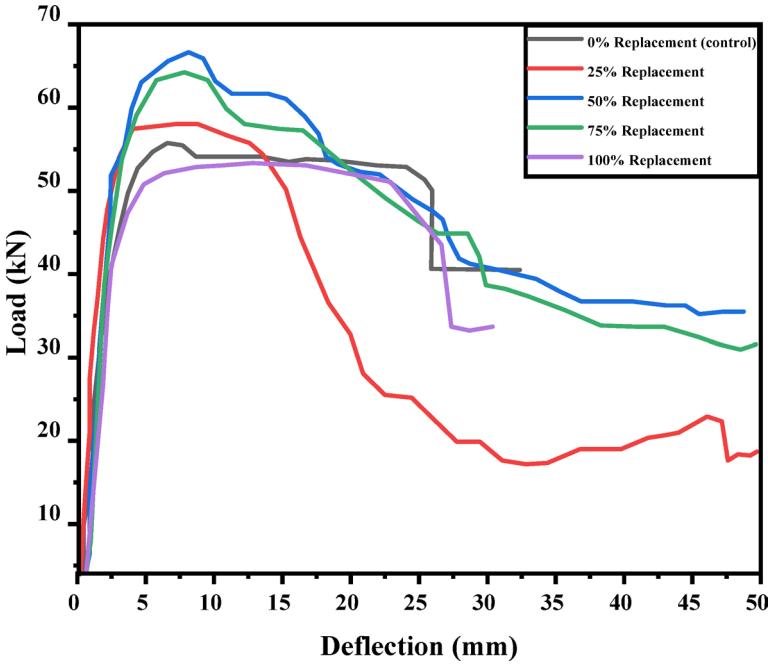

Fig. 14. Load–displacement curves of fine aggregate replacement.

Mix	Splitting tensile strength (psi)28 days	Shear strength (Psi)28 days
NCM (0%)	395.42	400.00
25% Slag	411.97	823.00
50% Slag	428.52	1137.67
75% Slag	456.12	1295.45
100% Slag	483.34	1446.67

Table 7. Average splitting tensile strength and shear strength results.

experienced earlier softening and greater deflection (9.0 mm), suggesting decreased stiffness and increased microstructural porosity due to the excessive slag content.

Similar trends were observed by Lai et al.[6], who identified the 33–50% range as optimal for structural concretes. These outcomes support the assertion that moderate slag replacement enhances flexural strength and ductility. Conversely, higher slag content may reduce workability and increase porosity, leading to premature post-peak decline, as evidenced by the behaviour of the 100% slag beam in this study. These results collectively suggest that partial slag replacement within the 25–50% range enhances both the flexural strength and ductility of reinforced concrete beams. However, full replacement (100%) leads to compromised performance, corroborating previous findings[3], and reinforcing the need for optimized slag utilization in structural concrete.

Splitting tensile strength (T)

The splitting tensile strength results for concrete mixes with varying slag replacement ratios are shown in Table 7; Fig. 15. The specimens incorporating 100% slag exhibited the highest strength, ranging from 465 to 502 psi across all three samples. This trend confirms the enhanced tensile capacity achieved through complete slag substitution. The 50% slag mix presented moderate strength values, between approximately 409 and 445 psi, showing an incremental improvement over the control mix but with some variation among samples. The normal concrete mix (0% slag) yielded the lowest tensile strengths, ranging from 380 to 410 psi. These results suggest that increasing slag content, particularly to 100%, positively influences the splitting tensile performance of concrete, potentially due to improved matrix densification and stronger particle bonding introduced by the slag material. Specimens subjected to the splitting tensile test failed by fracturing along the vertical diameter, consistent with indirect tensile failure. The crack propagation in slag-incorporated mixes appeared more uniform, suggesting a homogeneous distribution of stresses and a stronger interfacial transition zone, enabling more efficient transfer of tensile stresses.

Figure 16 illustrates the 3D surface plot of splitting tensile strength as a function of slag replacement percentage and sample number. The trend indicates a steady enhancement in tensile strength with increased slag content, peaking at 100% replacement across all samples. This improvement can be attributed to refined particle packing, improved interfacial bonding, and additional binding compounds generated during hydration.

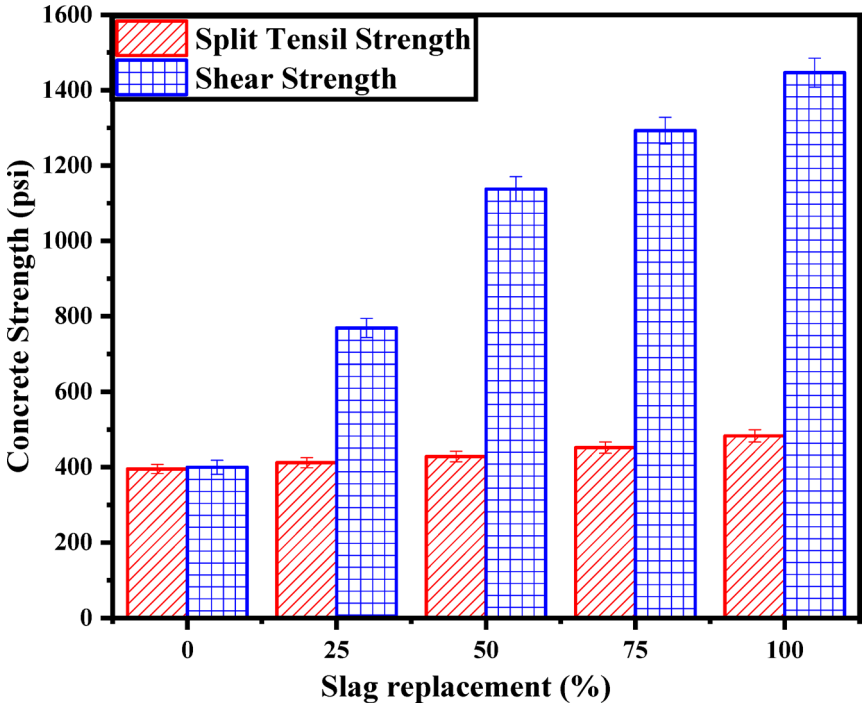

Fig. 15. Splitting tensile and Shear Strength results with varying slag replacement (%).

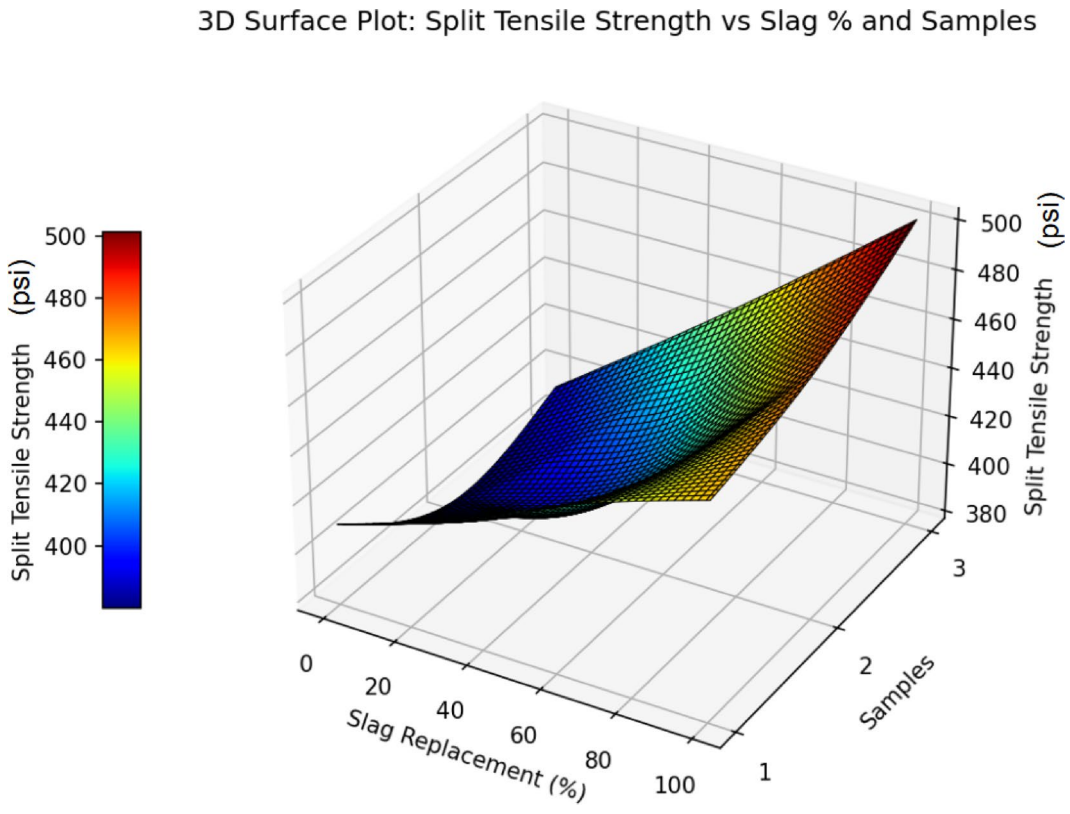

Fig. 16. The 3D Surface plot of splitting tensile strength results.

These effects collectively contribute to a denser and more cohesive concrete matrix, demonstrating that full slag substitution significantly benefits tensile performance.

Shear strength (Vc)

The shear strength of concrete beams incorporating varying percentages of steel slag as fine aggregate replacement was assessed and is presented in Fig. 15; Table 7. The results demonstrate a clear upward trend in shear strength with increasing slag content, suggesting enhanced matrix cohesion and improved interfacial bonding.

At 0% slag replacement (normal concrete mix), the average shear strength was approximately 400 psi. A modest improvement was observed at 25% slag replacement, with shear strength increasing to 725 psi, indicating that partial substitution begins to enhance the internal bonding within the concrete matrix. The strength further improved at 50% slag, reaching approximately 1137.67 psi, reflecting a significant gain in load-carrying capacity due to the synergistic effect of slag on paste densification and aggregate interlock. Beyond 50%, the 75% slag mix exhibited a continued increase in shear strength to around 1275 psi, and the 100% replacement achieved the highest shear capacity of 1446.67 psi. These results confirm that slag contributes positively to shear resistance, likely by refining pore structure and promoting denser particle packing. However, the rate of increase diminished beyond 75%, suggesting a point of diminishing returns. The incorporation of standard deviation bars also indicates that slag mixes yielded consistent performance with reduced variability, particularly at higher replacement levels. The shear strength tests primarily resulted in diagonal tension failure, with inclined cracks forming near the supports. The steel slag concrete beams, especially at higher replacement levels (75% and 100%), exhibited a more distributed cracking pattern and an increased load-carrying capacity before shear failure, indicating that the angularity and rough texture of steel slag significantly improved the aggregate interlock and the concrete's resistance to shear stresses.

These findings highlight the effectiveness of steel slag as a sustainable and performance-enhancing replacement material for fine aggregates, especially in structural applications where shear resistance is critical.

The 3D surface plot in Fig. 17 provides a clear visualization of how shear strength varies with different slag replacement percentages and sample numbers. The plot shows a consistent upward trend in shear strength as slag content increases from 0% to 100%. Notably, the surface gradient becomes steeper with higher replacement levels, indicating a significant improvement in shear performance, especially in samples 2 and 3. This enhancement can be attributed to the improved interfacial bonding and matrix densification provided by slag. The smooth colour gradient and surface curvature validate the uniformity and reliability of the results, supporting the conclusion that full slag replacement can effectively boost shear resistance in concrete beams.

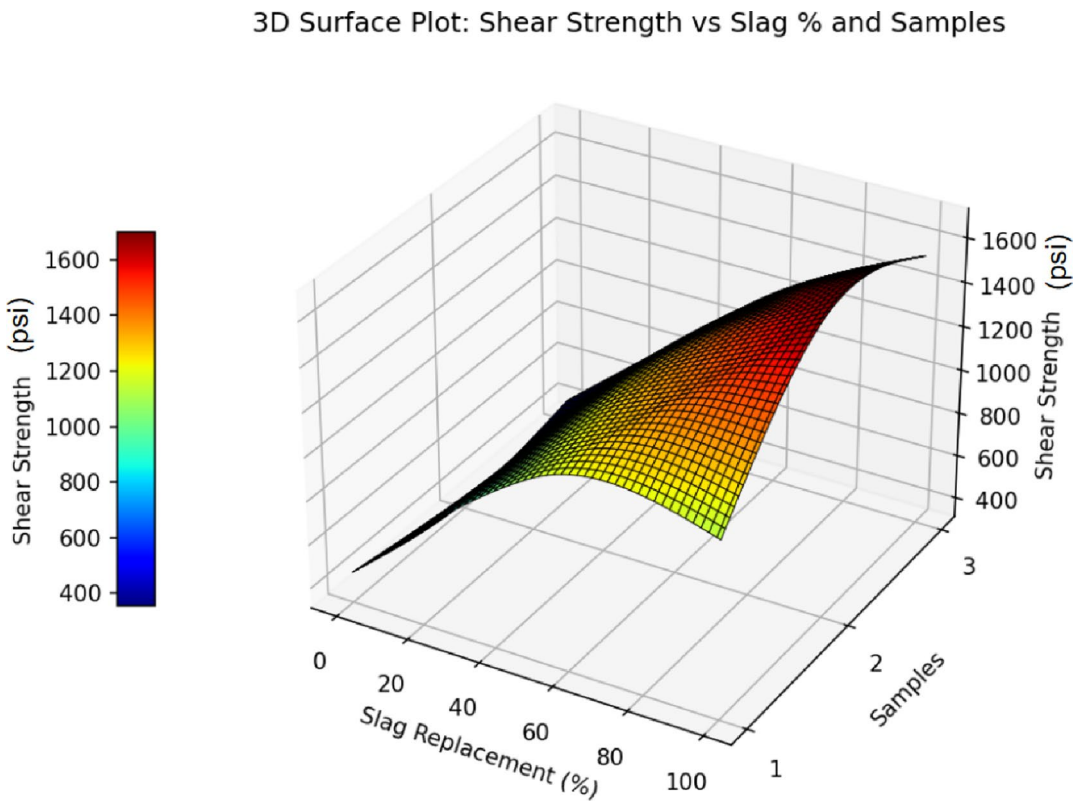

Fig. 17. The 3D Surface plot of shear strength results.

Residual compressive strength and mass change under H_2SO_4 (cylinders)

Compressive strength of immersed cylinders' $f_{c,n}$ was measured to EN 12390-3 at common ages (0, 28, 56, 90, 120 d); the 28-day strength of matched, unexposed companions provided the baseline $f_{c,0}$. Immersion followed the pH-controlled protocol in Sect. 2.5.7 (H_2SO_4, pH ≈ 1.0, 23 ± 2 °C; daily pH adjustment; solution renewal at reading ages). As shown in Fig. 18, strength decreases monotonically with exposure time for every replacement level (0% ≥ 25% ≥ 50% ≥ 75% ≥ 100% at each age). The decay is characterized by a pronounced early drop between 0 and 56 d followed by a slower decline from 90 to 120 d. At a fixed age, mixes with higher slag replacement retain lower residual capacity, consistent with faster degradation in the more heavily replaced concretes. Mechanistically, the early loss reflects decalcification of C-(A)-S-H and precipitation of gypsum/basanite in the corroded layer, which induces micro cracking and weakens the load bearing core. Once a stable residual core governs response, the rate of loss moderates at later ages. This time-dependent pattern and the need to evaluate both mass removal and mechanical capacity are consistent with sulfuric acid benchmarks in the literature, pH-controlled programs that track mass and strength for OPC/AAM mortars (Materials & Structures, 2017) and the 210-day AASC study that recommends a composite durability index under pH (1) exposure[43,64].

In line with that guidance, we interpret these strength results together with mass change. Mass change is reported as:

$$\Delta\, m\,(\%) = 100\frac{m_n - m_0}{m_0}\ (\text{loss is negative})$$

Figure 19 shows the mass change of the cylinders over time due to sulphuric-acid attack. All mixes show a monotonic decrease in mass with time. The drop is steeper from 0 to 56 d, followed by a slower decline from 90 to 120 d, consistent with rapid early surface softening/etching and a more gradual loss once a residual core governs. At any age, the 0% (NCM) mix exhibits the smallest loss, while the 100% slag mix shows the largest. The 25–75% band sits between these extremes; within that band, the 50% curve is slightly below (i.e., more negative than) 75% at later ages, but the separation is modest, well within what can arise from differences in transport and paste densification at intermediate replacement levels.

Under sulfuric acid, mass change (an ASTM-type indicator) tracks the net erosion/decalcification of the paste. pH-controlled programs consistently report monotonic mass loss with a pronounced early rate that later moderates; they also emphasize that mass change alone does not capture mechanical integrity, motivating the parallel analysis of residual strength and the use of a composite durability index. The results and protocol are aligned with the previous practices[43,64].

Durability index (DI_{2p})

To avoid single-metric bias, we aggregate strength retention and mass loss into the two-parameter durability index defined in Sect. (2.5.8). This multi-parameter approach follows sulphuric-acid durability programs that

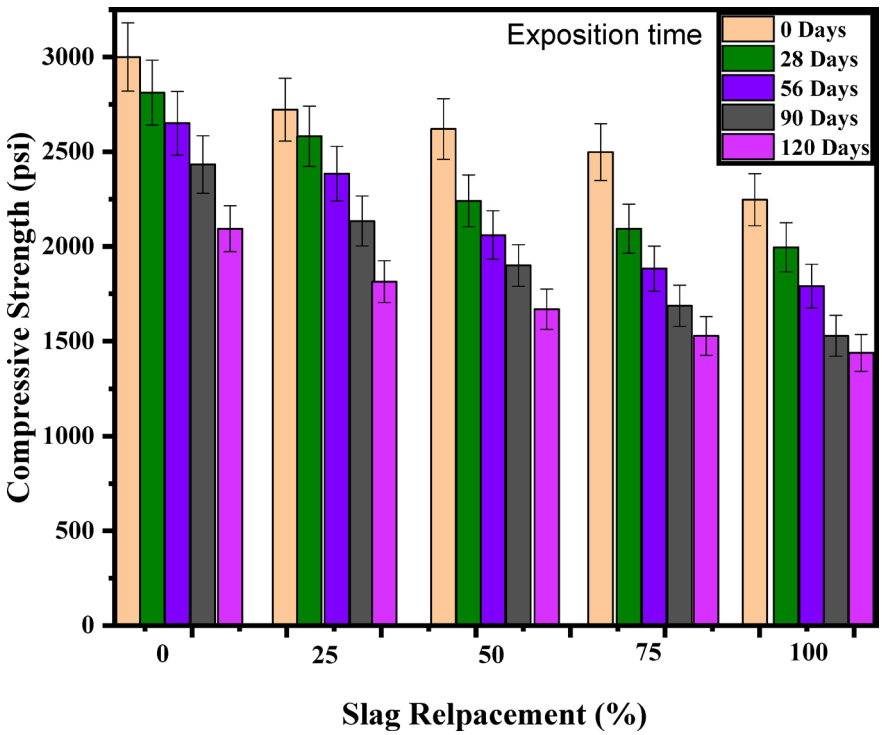

Fig. 18. Residual compressive strength (psi) of cylinder companions at 0, 25, 50, 75, 100% slag replacement after 0, 28, 56, 90, 120 days in H_2SO_4 (pH 1.0, 23 ± 2 °C).

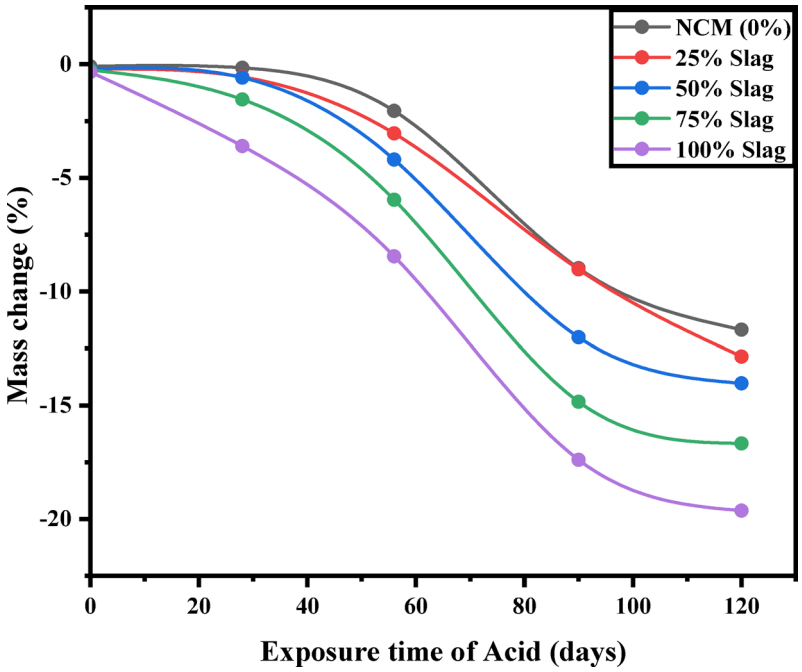

Fig. 19. Mass change (%, negative = loss) versus exposure time (0, 28, 56, 90, 120 days) for cylinder companions at 0, 25, 50, 75, 100% slag replacement in H_2SO_4 (pH 1.0, 23 ± 2 °C).

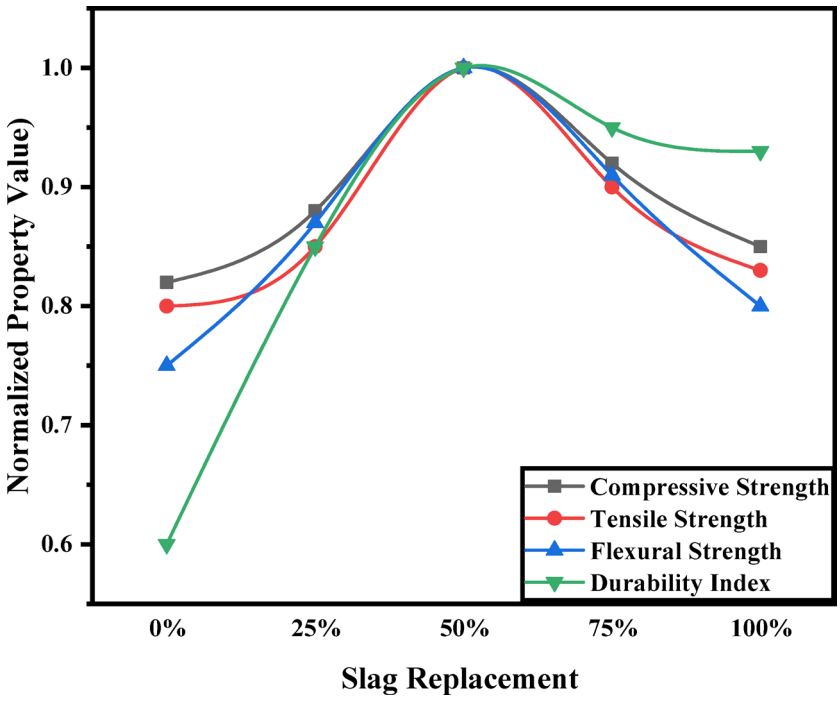

Fig. 20. Durability index evaluation.

recommend combining indicators under pH-controlled exposure rather than relying on a single measure such as mass or strength alone.

In addition to mechanical performance, the durability of slag-replaced concrete was evaluated using a normalized durability index, which integrates performance indicators such as resistance to acid attack and water absorption. As shown in Fig. 20, the durability index improved significantly with slag incorporation, peaking at 50% replacement. This enhancement is attributed to the refined pore structure and increased formation of secondary hydration products such as C–S–H and ettringite, which reduce permeability and improve chemical

resistance. Even at 75% replacement, durability remained high, indicating the potential of slag to replace cement without compromising long-term performance. The observed trend demonstrates that an optimal slag content can simultaneously enhance both strength and durability, supporting its use in sustainable concrete mix designs.

The observed sharper deviation of the composite Durability Index (DI_{2p}) curve in Fig. 20, compared to the more gradual changes typically seen in individual strength parameters (e.g., residual compressive strength alone), highlights its effectiveness in capturing the holistic degradation of concrete under acid attack. This sharper response is consistent with C–(A)–S–H decalcification and gypsum/basanite formation under H_2SO_4, which simultaneously increases erosion and reduces load-bearing capacity. This behaviour stems from the DI's formulation, which simultaneously accounts for both the mechanical strength loss and the physical material loss (weight loss). While concrete might initially experience a minor reduction in strength, the concurrent dissolution of the cementitious matrix leads to an increase in porosity and a reduction in mass. The multiplicative nature of the DI_{2p} amplifies the effect of these combined degradations, resulting in a more pronounced and sensitive indicator of overall material integrity. This suggests that the DI_{2p} more accurately reflects the combined impact of chemical and physical deterioration on the long-term performance of concrete in aggressive environments.

X-ray diffraction (XRD)

The XRD analysis of control mixes concrete samples before and after acid exposure, as illustrated in Fig. 21 shows changes in crystalline phases due to acid attack. The pre-acid exposure pattern (Fig. 21a) shows sharp and distinct peaks for key hydration products vital to the concrete's structural integrity, including a prominent Alite (C_3S) peak near 40° 2θ, indicative of un-hydrated clinker phases contributing to early strength, and a broad hump between 28°- 35°, 2θ corresponding to the C-S-H gel, the primary binder responsible for mechanical strength and durability. These pronounced peaks reflect a well-formed, intact cement matrix prior to acid exposure. After acid attack (Fig. 21b), there is a marked reduction in peak intensities, particularly the attenuation or disappearance of the Alite peak, signalling the progressive dissolution and degradation of un-hydrated cement phases. The C-S-H peak remains visible but with decreased intensity and broadening, suggesting partial degradation of the binding gel under acidic conditions. Residual peaks associated with Quartz (Q) around 22° and 60° 2θ indicate the chemical inertness and acid resistance of aggregate components. The overall smoother baseline and diminished peak sharpness confirm significant deterioration of the cement matrix and loss of crystalline order caused by acid exposure.

Figure 22 presents the XRD analysis of concrete samples containing 25% and 50% slag replacement, comparing crystalline phases before (pre-acid) and after (post-acid) acid exposure. The pre-acid pattern (Fig. 22a) exhibits distinct peaks for Portlandite (P), C-S-H, and Quartz (Q), indicating well-developed hydration products and the presence of inert aggregate phases. These peaks reflect the structural integrity and successful incorporation of slag into the cementitious matrix. Post-acid exposure (Fig. 22b) reveals a noticeable reduction in peak intensities, particularly for Portlandite and C-S-H, suggesting partial degradation of hydration products due to acid attack. However, the persistence of Quartz peaks highlights the chemical stability of the aggregate components. The relatively smoother baseline and diminished sharpness of peaks confirm matrix deterioration, although the slag inclusion appears to provide some resilience against acid-induced damage compared to traditional mixes. Interpolated behaviour for intermediate slag contents can also be inferred. For instance, the 25% slag mix likely shows moderate peak intensities between the CM and 50% slag samples. Post-acid exposure, it would exhibit reduced degradation compared to CM but more than the 50% mix, implying incremental improvement in durability with partial slag addition. Conversely, the 75% slag mix would demonstrate a closer resemblance to the 100% slag pattern shown in Fig. 23, with high retention of C-S-H and Quartz peaks and only minor attenuation, indicating substantial chemical resilience.

The pre-acid pattern (Fig. 23a) shows sharp, distinct peaks corresponding to hydration products such as Friedel's salt (F), C-S-H, and Quartz (Q), indicating a well-formed cementitious matrix with slag incorporation. The presence of Friedel's salt is characteristic of slag-based systems and contributes to improved chemical resistance. Post-acid exposure (Fig. 23b) reveals that while the intensities of the peaks slightly decrease, particularly for C-S-H, the overall pattern remains relatively stable. The persistence of Quartz peaks and the

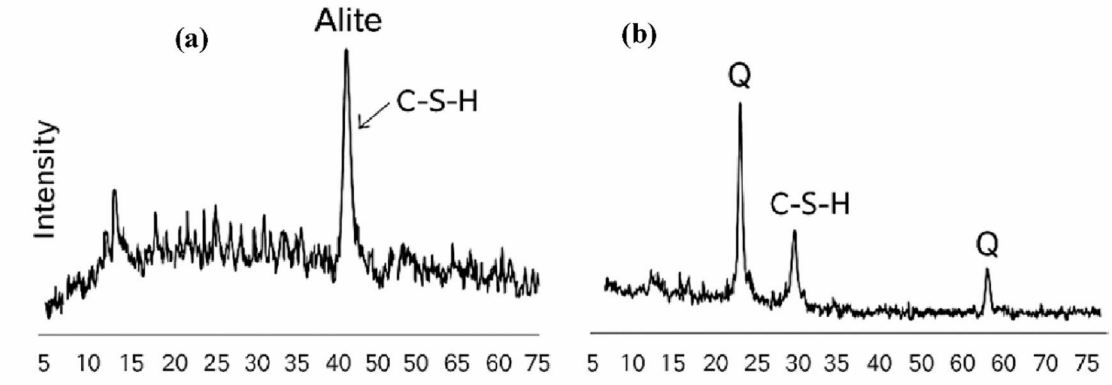

Fig. 21. XRD result of CM: (**a**) pre-acid and (**b**) post-acid attacks.

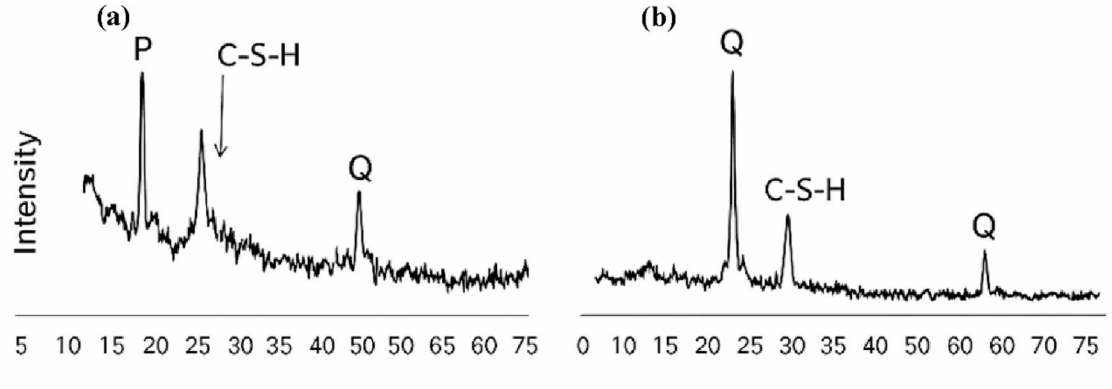

Fig. 22. XRD result of 25/50% slag Concrete: (**a**) pre-acid and (**b**) post-acid attacks.

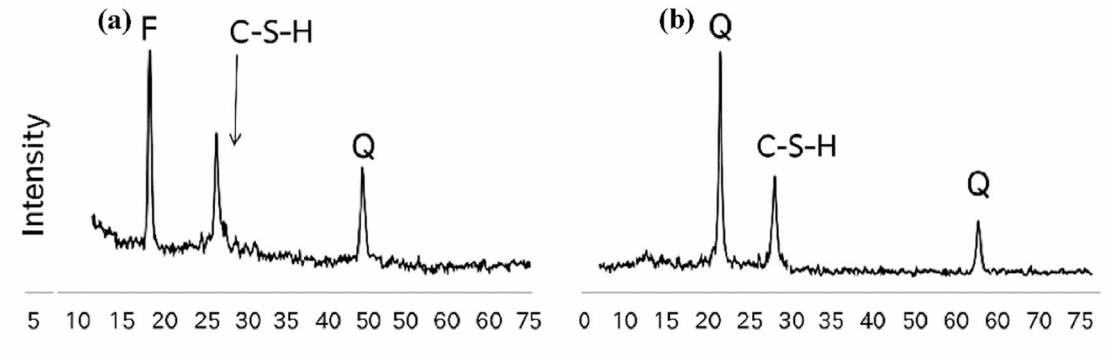

Fig. 23. XRD result of 75/100% slag Concrete: (**a**) pre-acid and (**b**) post-acid attacks.

retention of crystalline phases suggest that slag replacement enhances the concrete's resistance to acid attack by maintaining structural integrity and mitigating degradation compared to conventional mixes. This behaviour reflects the durability benefits of slag incorporation in aggressive environments.

In the control mix, the distinct crystalline peaks of Alite (C_3S) and Portlandite ($Ca(OH)_2$) were prominent pre-acid exposure, alongside the broad C-S-H hump. After the acid attack, a significant reduction in the intensity of these crystalline phases was observed, indicating their dissolution, while the C-S-H hump also broadened and diminished, signifying its decalcification and degradation. In contrast, slag-blended concretes (25% to 100% replacement) showed a better retention of the C-S-H hump and crystalline Quartz peaks even after acid exposure. This suggests that slag incorporation mitigates the degradation of the amorphous C-S-H gel and preserves the integrity of the inert aggregate phases, contributing to enhanced chemical resistance. The continued presence of Friedel's salt in higher slag mixes further indicates mechanisms that enhance resistance to chloride or sulphate ingress, supporting the overall durability. Overall, the XRD analysis demonstrates that increasing slag replacement enhances the acid resistance and durability of concrete. The control mix exhibits pronounced degradation of hydration phases such as Alite and C-S-H after acid exposure. In contrast, samples with 25%, 50%, 75%, and 100% slag replacement show progressively improved stability of crystalline phases, especially the persistence of C-S-H and Quartz peaks, indicating less matrix deterioration. The retention of Friedel's salt and Quartz in higher slag mixes suggests that slag incorporation mitigates acid-induced damage by preserving the structural integrity of the cementitious matrix, with 100% slag showing the most chemical resilience under aggressive conditions.

Conclusion and recommendation

Conclusion

This study comprehensively evaluated the viability of utilizing steel slag as a sustainable substitute for fine aggregates in concrete. The key findings demonstrate that steel slag not only serves as a competent replacement but also significantly enhances the performance characteristics of concrete, particularly in demanding environments.

- The experimental results revealed that a 50% replacement of natural sand with steel slag yielded an optimal balance of properties, achieving a 10.5% increase in 28-day compressive strength alongside superior splitting tensile and flexural strength compared to the control mix. This suggests an enhanced microstructure and im-

proved bonding within the concrete matrix. Notably, even the 100% replacement mix exhibited exceptional performance in specific areas, recording the highest splitting tensile strength (483.34 psi) and shear strength (1446.67 psi), which indicates a high deformation capacity beneficial for applications requiring shear resistance.

- Beyond mechanical performance, the durability assessment proved critical. A novel composite durability index (DI), which integrates residual strength and material loss, confirms the enhanced chemical resistance of slag-incorporated concrete. The 50% slag mix significantly outperformed the control, achieving a DI of 84.3% compared to 73.8% during acid exposure tests. This superior resilience was further validated by XRD analysis, which confirmed the persistence of vital cementitious phases, such as C-S-H and quartz, indicating a more stable and chemically resistant matrix.
- Practical Implications: The incorporation of steel slag presents a dual advantage: it enhances the mechanical and durability properties of concrete while promoting sustainability by reducing the consumption of natural sand. Based on the overall performance, a replacement level of 25–60% is recommended as the most favourable range. This proportion offers an ideal synergy of high strength, improved ductility, and exceptional durability, making it particularly suitable for structural applications in chemically aggressive environments. Potential applications include wastewater treatment facilities, industrial flooring, foundations in contaminated soil, and marine or coastal structures.

In conclusion, steel slag is established as a high-performance, eco-friendly alternative to fine aggregates, contributing to the development of more resilient and sustainable construction materials.

Future research and limitations

While this study provides a comprehensive laboratory-scale evaluation of steel slag as a fine aggregate replacement, certain limitations must be acknowledged. The experimental program primarily focused on the mechanical properties of early age (28-day) specimens and a specific accelerated acid exposure regime. To better understand the potential of steel slag concrete, future studies should investigate its long-term durability under a range of real-world conditions, including sulfate attack, freeze-thaw cycles, and thermal stress. Additionally, the constant water-cement ratio used across all mixes did not account for variations in workability or effective water absorption due to differing slag contents, which may influence field performance. Future research should address these factors to more effectively simulate real-world applications. Although qualitative, detailed quantitative phase analysis (QPA) of microstructural changes, using techniques such as Rietveld refinement, was beyond the scope of this study, further exploration in this area could provide deeper insights into the material's stability and long-term performance.

Another key limitation is the lack of specific provisions for steel slag in established building design codes, such as ACI 318[65] and Eurocode 2[66]. The widespread adoption of steel slag in structural concrete will require project-specific approvals or performance-based design approaches. Further research is needed to validate the proposed mixes through large-scale experimental testing (e.g., tests on reinforced concrete beams or walls under specific loading conditions) and advanced numerical modelling. In terms of future research, studies should focus on optimizing mix designs, conducting life cycle assessments (LCA) to evaluate the environmental impact of using steel slag, and investigating the material's fire resistance and compatibility with other supplementary cementitious materials (SCMs). These efforts will provide crucial data to inform sustainable, high-performance concrete solutions.

Data availability

The datasets used and/or analyzed during the current study are available from the corresponding author on reasonable request.

Received: 31 July 2025; Accepted: 15 October 2025
Published online: 20 November 2025

References

1. Chow, R. K. K., Yip, S. W. S. & Kwan, A. K. H. Processing crushed rock fine to produce manufactured sand for improving overall performance of concrete. *HKIE Trans.* **20**, 240–249 (2013).
2. Mundra, S., Sindhi, P. R., Chandwani, V., Nagar, R. & Agrawal, V. Crushed rock sand–An economical and ecological alternative to natural sand to optimize concrete mix. *Perspect. Sci.* **8**, 345–347 (2016).
3. Mekonen, T. B., Alene, T. E., Alem, Y. A. & Nebiyu, W. M. Influence of steel slag as a partial replacement of aggregate on performance of reinforced concrete beam. *Int. J. Concrete Struct. Mater.* **18**, 56 (2024).
4. Al-Jabri, K. S., Al-Saidy, A. H. & Taha, R. Effect of copper slag as a fine aggregate on the properties of cement mortars and concrete. *Constr. Build. Mater.* **25**, 933–938 (2011).
5. Valcuende, M., Benito, F., Parra, C. & Miñano, I. Shrinkage of self-compacting concrete made with blast furnace slag as fine aggregate. *Constr. Build. Mater.* **76**, 1–9 (2015).
6. Guo, Y., Xie, J., Zheng, W. & Li, J. Effects of steel slag as fine aggregate on static and impact behaviours of concrete. *Constr. Build. Mater.* **192**, 194–201 (2018).
7. Surangi, M. L. C., Julnipitawong, P., Tangtermsirikul, S., Ohgi, Y. & Ishii, Y. Using fly Ash as a partial replacement for fine aggregate in concrete and its effects on concrete properties under different curing temperatures. *ASEAN Eng. J.* **10** (2020).
8. Das, K. K., Lam, E. S. S. & Tang, H. H. Partial replacement of cement by ground granulated blast furnace slag and silica fume in two-stage concrete (preplaced aggregate concrete). *Struct. Concrete.* **22**, E466–E473 (2021).
9. Khan, K. et al. Effective use of micro-silica extracted from rice husk Ash for the production of high-performance and sustainable cement mortar. *Constr. Build. Mater.* **258**, 119589 (2020).
10. Ullah, M. F. et al. Mechanical and environmental performance of sugarcane Bagasse Ash from Khyber Pakhtunkhwa in sustainable concrete. *Sci. Rep.* **15**, 24571 (2025).

11. Keerio, M. A. et al. Effect of silica fume as cementitious material and waste glass as fine aggregate replacement constituent on selected properties of concrete. *Silicon* **14**, 165–176 (2022).
12. Peng, Y. et al. Evaluation framework for bitumen-aggregate interfacial adhesion incorporating pull-off test and fluorescence tracing method. *Constr. Build. Mater.* **451**, 138773 (2024).
13. Huang, H., Guo, M., Zhang, W. & Huang, M. Seismic behavior of strengthened RC columns under combined loadings. *J. Bridge Eng.* **27**, 05022005 (2022).
14. Sun, L. et al. Experimental investigation on the bond performance of sea sand coral concrete with FRP bar reinforcement for marine environments. *Adv. Struct. Eng.* **26**, 533–546 (2023).
15. Maganti, T. R., Kandikuppa, C. S., Gopireddy, H. K. R., Dugalam, R. & Boddepalli, K. R. Enhanced compressive strength and impact resistance in hybrid fiber reinforced ternary-blended alkali-activated concrete: An experimental, Weibull analysis and finite element simulation. *Composites Part. C* **100629** (2025).
16. Maganti, T. R. & Boddepalli, K. R. Synergistic enhancement of compressive strength and impact resistance in alkali-activated fiber-reinforced concrete through silica fume and hybrid fiber integration. *Constr. Build. Mater.* **471**, 140702 (2025).
17. Maganti, T. R. & Boddepalli, K. R. Optimization of mechanical and impact resistance of high strength glass fiber reinforced alkali activated concrete containing silica fume: an experimental and response surface methodology approach. *Case Stud. Constr. Mater.* **22**, e04343 (2025).
18. Sankh, A. C., Biradar, P. M., Naghathan, S. J. & Ishwargol M. B. 59–66 .
19. El Machi, A. et al. Recycling of mine wastes in the concrete industry: a review. *Buildings* **14**, 1508 (2024).
20. Xie, Y., Far, H., Mortazavi, M. & El-Sherbeeny, A. M. Improving the mechanical properties of concrete mixtures by shape memory alloy fibers and silica fume. *Buildings* **14**, 1709 (2024).
21. Fernandes, F. A., d., S., Fernandes, T. F., d., S. & Rossignolo, J. A. Production of glass foam in a microwave oven using Agro-Industrial waste as Raw material. *Buildings* **14**, 1643 (2024).
22. Gandhi, S. et al. Analysis of potential incorporation of waste into asphalt pavements. *Mater. Today* (2024).
23. Bahoria, B. V. et al. Verification of the mechanical behavior of concrete with partial replacement of the fiber resulting from tire retreading. *Mater. Today* (2024).
24. Santhosh, N. et al. Mechanical properties studies on rubber composites reinforced with acacia caesia fibre. *Mater. Today: Proc.* **72**, 3172–3176 (2023).
25. Wijaya, R. & Astutiningsih, S. Studi literatur potensi Pemanfaatan Terak Nikel (Slag Nikel) Sebagai Agregat Pada mortar Dan Beton. *Bentang: Jurnal Teoritis dan. Terapan Bidang Rekayasa Sipil.* **9**, 93–100 (2021).
26. Mustika, W., Salain, I. & Sudarsana, I. K. *Penggunaan Terak Nikel Sebagai Agregat Dalam Campuran Beton* (Program Magister Studi Teknik Sipil, 2016).
27. Edwin, R. S., Ngii, E., Talanipa, R., Masud, F. & Sriyani, R. 1 edn 01 (IOP Publishing, 2014).
28. Yang, L. et al. Three-dimensional concrete printing technology from a rheology perspective: a review. *Adv. Cem. Res.* **36**, 567–586 (2024).
29. Wang, K., Chen, Z., Wang, Z., Chen, Q. & Ma, D. Critical dynamic stress and cumulative plastic deformation of calcareous sand filler based on shakedown theory. *J. Mar. Sci. Eng.* **11**, 195 (2023).
30. Liu, F. et al. *Improved Thermal performance, Frost resistance, and Pore Structure of cement–based Composites by Binary Modification with mPCMs/nano–SiO2* 137166 (Energy, 2025).
31. Wang, J., Wu, Z., Han, J., Wang, G. & Lv, S. Experimental study on axial load-bearing capacity of grout-lifted compressible concrete-filled steel tube composite column. *Tunn. Undergr. Space Technol.* **165**, 106864 (2025).
32. Zhu, J. F., Wang, Z. Q., Tao, Y. L., Ju, L. Y. & Yang, H. Macro–micro investigation on stabilization sludge as subgrade filler by the ternary blending of steel slag and fly Ash and calcium carbide residue. *J. Clean. Prod.* **447**, 141496 (2024).
33. Shi, T. et al. *Fracture Toughness of Recycled Carbon Fibers Reinforced Cement Mortar and its Environmental Impact Assessment* e04866 (Case Studies in Construction Materials, 2025).
34. Niu, Y., Wang, W., Su, Y., Jia, F. & Long, X. Plastic damage prediction of concrete under compression based on deep learning. *Acta Mech.* **235**, 255–266 (2024).
35. Han, F., Zhang, Z., Wang, D. & Yan, P. Hydration heat evolution and kinetics of blended cement containing steel slag at different temperatures. *Thermochim. Acta*. **605**, 43–51 (2015).
36. December 2022 crude steel production and 2022 global crude steel production totals (2023).
37. Yi, H. et al. An overview of utilization of steel slag. *Procedia Environ. Sci.* **16**, 791–801 (2012).
38. Ren, Z. & Li, D. Application of steel slag as an aggregate in concrete production: a review. *Materials* **16**, 5841 (2023).
39. Guo, J., Bao, Y. & Wang, M. Steel slag in china: Treatment, recycling, and management. *Waste Manage.* **78**, 318–330 (2018).
40. Najm, O., El-Hassan, H. & El-Dieb, A. Ladle slag characteristics and use in mortar and concrete: A comprehensive review. *J. Clean. Prod.* **288**, 125584 (2021).
41. Es-samlali, L., El Haloui, Y., Oudrhiri-Hassani, F., Tlidi, A. & Bekri, A. Natural aggregate substitution by steel slag waste for concrete manufacturing. *GEOMATE J.* **26**, 61–72 (2024).
42. Mehta, P. K. & Monteiro, P. J. *M. Concrete microstructure, properties, and Materials* (McGraw-hill, 2006).
43. Nasrollahzadeh, K. & Rostami, M. Experimental investigation on durability of One-Part and Two-Part Alkali-Activated slag concretes in sulfuric acid environment: Development of a durability index and CO2 emission assessment. *Arab. J. Sci. Eng.* 1–28 (2025).
44. Maganti, T. R., Gopireddy, H. K. R. & Boddepalli, K. R. Enhanced flexural performance and crack control in hybrid fiber ECC-ACC beams. *Ain Shams Eng. J.* **16**, 103451 (2025).
45. Maganti, T. R. & Boddepalli, K. R. Mechanical and microstructural properties of sustainable ternary blended alkali-activated concrete. *Next Sustain.* **6**, 100122 (2025).
46. Mitwally, M. E., Elnemr, A., Shash, A. & Babiker, A. Utilization of steel slag as partial replacement for coarse aggregate in concrete. *Innovative Infrastructure Solutions*. **9**, 175 (2024).
47. Afaque, M., Khan, R. A. & Roy, S. Durability and strength enhancement in concrete using steel slag as fine aggregate replacement. *Mater. Circular Econ.* **6**, 46 (2024).
48. Astm, A. C150/C150M-17, standard specification for Portland cement. Am. Soc. Test. Mater. (2017).
49. Astm, C. Standard test method for sieve analysis of fine and coarse aggregates. *ASTM C* 136–106 (2006).
50. Anson-Cartwright, M. Optimization of aggregate gradation combinations to improve concrete sustainability (2011).
51. Tangadagi, R. B., Manjunatha, M., Bharath, A. & Preethi, S. Utilization of steel slag as an eco-friendly material in concrete for construction. *J. Green. Eng.* **10**, 2408–2419 (2020).
52. Suri, N. & Babu, Y. A. Experimental investigations on partial replacement of steel slag as coarse aggregates and eco sand as fine aggregate. *Int. J. Civil Eng. Technol.* **7** (2016).
53. Standard test method. for the compressive strength of concrete cylinder, ASTM-C39/C39M (2020).
54. Astm, C. Standard test method for flexural strength of concrete (using simple beam with center-point loading) (2002).
55. ASTM C496/C496M-17. Test method for splitting tensile strength of cylindrical concrete specimens. ASTM International, West Conshohocken, PA (2017).
56. Taylor, H. F. *W. Cement Chemistry* Vol. 2 (Thomas Telford London, 1997).
57. Shayan, A., Diggins, R. & Ivanusec, I. Effectiveness of fly Ash in preventing deleterious expansion due to alkali-aggregate reaction in normal and steam-cured concrete. *Cem. Concr. Res.* **26**, 153–164 (1996).

58. Zhang, Y., Sun, Q. & Geng, J. Microstructural characterization of limestone exposed to heat with XRD, SEM and TG-DSC. *Mater. Charact.* **134**, 285–295 (2017).
59. Chukhchin, D. G., Malkov, A. V., Tyshkunova, I. V., Mayer, L. V. & Novozhilov, E. V. Diffractometric method for determining the degree of crystallinity of materials. *Crystallogr. Rep.* **61**, 371–375 (2016).
60. Chopperla, K. S. T. et al. Unified durability guidance in ACI committee documents. *ACI Mater. J.* **119**, 29–41 (2022).
61. Wang, Y. et al. Study of acidic degradation of alkali-activated materials using synthetic C-(N)-ASH and NASH gels. *Compos. Part. B: Eng.* **230**, 109510 (2022).
62. Hendi, A., Behravan, A., Mostofinejad, D., Kharazian, H. A. & Sedaghatdoost, A. Performance of two types of concrete containing waste silica sources under MgSO4 attack evaluated by durability index. *Constr. Build. Mater.* **241**, 118140 (2020).
63. Shetty, M. S. *Concrete Technology Theory and Practice* (Chand S. and Company LTD. New Delhi, 2005).
64. Aliques-Granero, J., Tognonvi, T. M. & Tagnit-Hamou, A. Durability test methods and their application to aams: case of sulfuric-acid resistance. *Mater. Struct.* **50**, 36 (2017).
65. Aci, A. *C. I. 318 – 19 & ACI 318R-19: Building Code Requirements for Structural Concrete and Commentary* (American Concrete Institute, 2019).
66. Européen, C. *Eurocode 2: Design of Concrete structures—Part 1–1: General Rules and Rules for Buildings* 37 (British Standard Institution, 2004).

Acknowledgements

The authors gratefully acknowledge the support provided by the structural engineering laboratory team at Tongji University for their assistance with experimental testing.

Author contributions

Adnan Khan, Muhammad Luqman, Xu Jun, Muhammad Fahad Ullah, Abdullah Alzlfawi, Mahmood Ahmad, and Zsolt Toth were responsible for the conceptualization and design of the study. Adnan Khan and Muhammad Luqman conducted data collection and analysis. Xu Jun and Muhammad Fahad Ullah prepared the initial draft of the manuscript. Abdullah Alzlfawi, Mahmood Ahmad, and Zsolt Toth provided critical reviews and revisions to the manuscript. All authors reviewed and approved the final version of the manuscript for submission.

Funding

The authors declare that no funds, grants, or other support were received during the preparation of this manuscript. Furthermore, the Article Processing Charges (APC) of this project are paid by the University of Sopron, Hungary.

Declarations

Competing interests

The authors declare no competing interests.

Additional information

Correspondence and requests for materials should be addressed to Z.T.